Letter

Tunable molecular interactions near an atomic Feshbach resonance: Stability and collapse of a molecular Bose-Einstein condensate

Zhiqiang Wang [1,2,3,4,*] Ke Wang [4] Zhendong Zhang [5,6] Qijin Chen [1,2,3] Cheng Chin [4,7] and K. Levin [4]

[1]Hefei National Research Center for Physical Sciences at the Microscale and School of Physical Sciences, University of Science and Technology of China, Hefei, Anhui 230026, China

[2]Shanghai Research Center for Quantum Science and CAS Center for Excellence in Quantum Information and Quantum Physics, University of Science and Technology of China, Shanghai 201315, China

[3]Hefei National Laboratory, University of Science and Technology of China, Hefei 230088, China

[4]Department of Physics and James Franck Institute, University of Chicago, Chicago, Illinois 60637, USA

[5]E. L. Ginzton Laboratory and Department of Applied Physics, Stanford University, Stanford, California 94305, USA

[6]Department of Physics and Hong Kong Institute of Quantum Science and Technology, The University of Hong Kong, Hong Kong, China

[7]Enrico Fermi Institute, University of Chicago, Chicago, Illinois 60637, USA

(Received 27 April 2025; accepted 5 December 2025; published 29 December 2025)

Understanding and controlling interactions of ultracold molecules is a cornerstone of quantum chemistry. While the laboratory creation of degenerate molecular gases comprised of bosonic atoms has unlocked powerful platforms for quantum simulation, progress is limited by the absence of a robust theoretical framework for characterizing intermolecular interactions. This is in stark contrast to the situation for Fermi gases. In this Letter, we present such a framework providing universal expressions for these molecular scattering lengths as functions of experimentally measurable quantities. Our discoveries are crucial for understanding molecular condensate formation. Calculations of the compressibility reveal that a sign change in such molecular scattering lengths is directly correlated with the instability of these condensates. These results offer fresh insight with broad applications for atomic, molecular, and condensed matter physics, as well as quantum chemistry.

DOI: 10.1103/r2gt-gcyt

Introduction. Molecular condensates of bosonic atoms represent a key frontier in physics, offering a path to discover states of matter and quantum phase transitions [1–4]. The use of Feshbach resonances [5], particularly through magnetoassociation, has revolutionized our ability to create stable diatomic molecules from ultracold atomic pairs. This has allowed for the preparation of equilibrium molecular condensates [6,7].

Despite this progress, bosonic systems face significant challenges. Condensates become unstable near a resonance, as they experience particle loss and heating due to three-body recombination [8–11]. Feshbach interactions can add to this condensate destabilization when they introduce an attractive force between molecules. Such instabilities contrast sharply with two-component Fermi gases, where the Pauli exclusion principle [12,13] allows for the robust formation of stable molecular condensates. The stability in fermionic systems has enabled an extensive exploration of the Bardeen-Cooper-Schrieffer (BCS) to Bose-Einstein-condensation (BEC) crossover [14–17], a level of understanding that has yet to be replicated with bosons. Here, BCS-BEC crossover refers to a superfluid undergoing a smooth evolution, with increasing interaction strength, from large, overlapping Cooper pairs to tightly bound diatomic molecules.

In this paper, we address this critical issue of bosonic molecular condensate instability by examining the molecule-molecule scattering length. Our approach is inspired by atomic condensates, where the two-body s-wave scattering length is typically described by the following equation:

$$a_s = a_{\rm bg}\left(1 - \frac{\Delta B}{B - B_0}\right). \tag{1}$$

Here, B_0 is the resonance value of the magnetic field B, ΔB is the resonance width, and $a_{\rm bg}$ is the atomic s-wave background scattering length. The leading-order contribution to a_s due to the Feshbach coupling can be visualized as in Fig. 1(a) [18].

It is well known that atomic condensates collapse when a_s becomes negative. This typically happens when the magnetic field B is above the resonance, specifically within the range $B_0 < B < B_0 + \Delta B$ (assuming a positive atomic background scattering length, $a_{\rm bg} > 0$). For concreteness, here we assume $\Delta B > 0$, so that the bare molecules' energy drops below the atom continuum when the magnetic field is below resonance ($B < B_0$) [19]. What has not been widely appreciated is that Feshbach coupling can also modify the scattering properties of molecules, which can lead to the instability of a

*Contact author: wzhiqustc@ustc.edu.cn

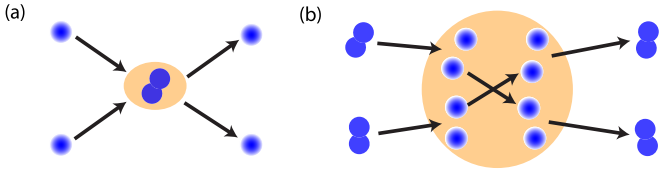

FIG. 1. Scattering due to atomic Feshbach coupling: (a) Leading-order scattering process contributing to the resonant term in the atomic scattering length, a_s [Eq. (1)]. Two incoming atoms (single blue circles) temporarily combine into a molecule (two attached circles) via Feshbach coupling, and then dissociate into two outgoing free atoms. The orange region represents virtual processes. (b) Corresponding leading-order contribution to the molecular scattering length, $a_{\rm mm}$, near the resonance. Here, two molecules approach each other and temporarily break up into four free atoms, which then propagate, interact, and recombine into two molecules. Similar to panel (a), this process universally depends on the Feshbach coupling but is of higher order in the coupling strength.

molecular Bose-Einstein condensate. Understanding this important effect is central to our investigation.

In this Letter, we demonstrate how Feshbach resonances dramatically alter the intermolecular scattering length and consequently the behavior of bosonic molecular condensates, mirroring their profound effect in atomic systems. Crucially, this tunability can drive molecular condensates into instability when this scattering length (called $a_{\rm mm}$ at zero and $a_{\rm mm}^{\rm eff}$ at finite density) becomes negative. Notable is a rather pronounced density dependence found in $a_{\rm mm}^{\rm eff}$ for narrow resonances, which arises from many-body effects and introduces additional complexity; only in the limit of very wide Feshbach resonances does $a_{\rm mm}^{\rm eff}$ simplify, converging with the two-body scattering length $a_{\rm mm}$.

The accurate determination of both the fundamental molecular scattering length ($a_{\rm mm}$) and the density-dependent effective scattering length ($a_{\rm mm}^{\rm eff}$) presents a significant theoretical challenge. As Fig. 1(b) illustrates, even a leading-order intermolecular scattering process can be considerably more complex as it involves higher order in Feshbach coupling strength than what is seen in simpler atomic systems [Fig. 1(a)]. Additionally, we also need to precisely account for background interactions between atoms and molecules.

Summary of main results. Our theoretical framework employs a two-channel variational wave function treatment to systematically analyze the system's compressibility and, from it, deduce the crucial scattering lengths. We begin by presenting general insights into the zero-temperature stability phase diagrams presented in Fig. 2, which are determined through numerical calculations of the compressibility $\kappa = dn/d\mu$.

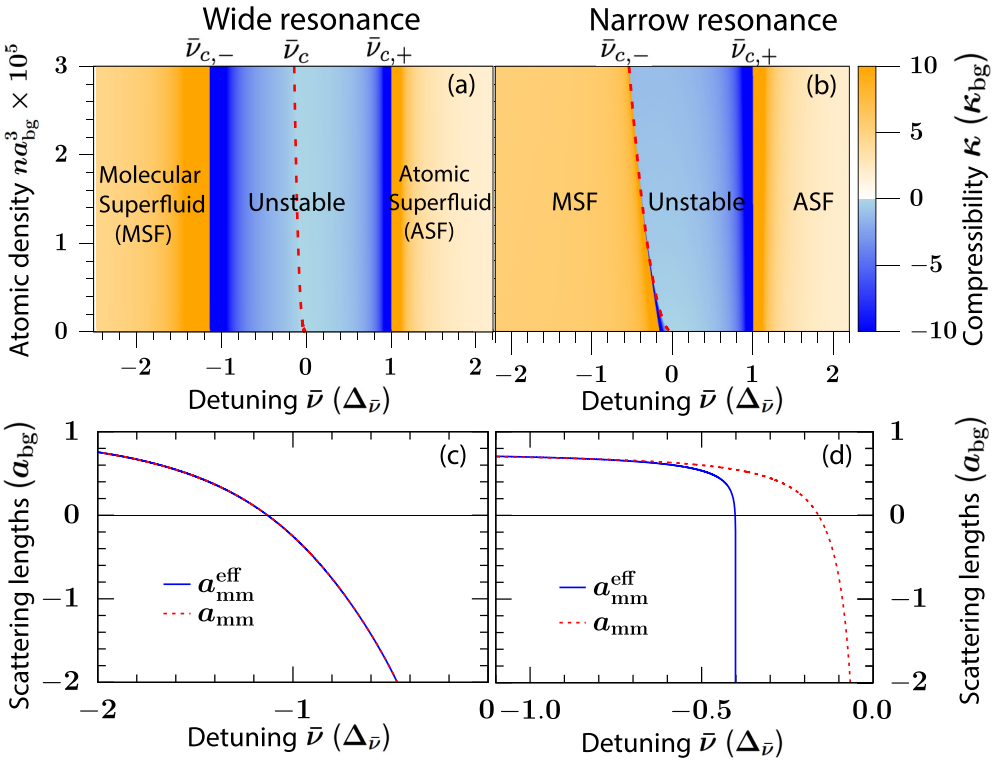

FIG. 2. Phase diagrams and molecular scattering lengths. Ground-state stability phase diagrams for (a) wide and (b) narrow resonances, showing compressibility κ [normalized by $\kappa_{\rm bg} = m_1/(4\pi\hbar^2 a_{\rm bg})$] as a function of atom number density n and of detuning $\bar{\nu} = \Delta\mu_m(B - B_0)$ (normalized by resonance width $\Delta_{\bar{\nu}} = \Delta\mu_m \Delta B$). Orange indicates stable regions ($\kappa > 0$), and blue indicates unstable regions. The atomic condensate is present only in the atomic superfluid (ASF) phase, while the molecular condensate is present in both ASF and molecular superfluid (MSF) phases. Red dashed lines denote the quantum critical point $\bar{\nu}_c(n)$ separating ASF from MSF, while $\bar{\nu}_{c,-}$ and $\bar{\nu}_{c,+}$ mark boundaries between unstable and stable regions. (c), (d) Corresponding two-body molecular scattering length $a_{\rm mm}$, and its many-body analog $a_{\rm mm}^{\rm eff}(n)$ for $na_{\rm bg}^3 = 1.68 \times 10^{-5}$. Parameters for the narrow resonance [panels (b and (d)] are from the ^{133}Cs resonance at $B_0 = 19.849$ G [6,7,20]. For the wide resonance [panels (a) and (c)], $\Delta_{\bar{\nu}}$ is increased by 10^2 times relative to panels (b) and (d).

Figures 2(a) and 2(b) show the zero-temperature stability phase diagrams for both a wide and a narrow resonance, in terms of density n on the vertical axis and detuning $\bar{\nu}$ on the horizontal axis. Both panels indicate a stable molecular superfluid phase at large negative detuning, a stable atomic superfluid phase at large positive detuning, and an unstable region in between, where the compressibility becomes negative: $\kappa < 0$. The boundaries of this unstable region are marked by the detunings $\bar{\nu}_{c,+}$ and $\bar{\nu}_{c,-}$. In Figs. 2(c) and 2(d), we plot both our calculated two-body scattering length, $a_{\rm mm}$, and its many-body analog $a^{\rm eff}_{\rm mm}(n)$.

Note a striking similarity between panels (a) and (b) of Fig. 2 on the atomic side. For both narrow and wide resonances, the phase boundary of the unstable region is essentially dictated by the sign change of the two-body atomic scattering length, a_s. This means that in both scenarios, the upper boundary detuning of the unstable regime, $\bar{\nu}_{c,+}$, remains nearly independent of density.

In contrast, the behavior of the compressibility on the molecular side of the phase diagrams in Figs. 2(a) and 2(b) reveals a significant difference between wide and narrow resonances. We summarize our key observations:

(1) *Wide resonance case with density-independent stability*. In the case of wide resonances, the entire unstable region shows very little dependence on density. This is a significant finding because it means we can roughly characterize the molecular condensate's stability using just a two-body scattering length, similarly to how we treat atomic condensates. Figure 2(c) confirms this, showing that $a^{\rm eff}_{\rm mm}(n)$ is nearly equivalent to $a_{\rm mm}$, and importantly, $a_{\rm mm}$ itself changes sign at the instability onset detuning, $\bar{\nu}_{c,-}$, in Fig. 2(a).

(2) *Narrow resonance case with strong density dependence*. In contrast, for narrow resonances, the lower boundary detuning, $\bar{\nu}_{c,-}$, of the unstable region in Fig. 2(b) is highly dependent on density. Here, it is the density-dependent many-body scattering length, $a^{\rm eff}_{\rm mm}$, not the two-body $a_{\rm mm}$, that changes sign at this instability boundary, as clearly shown in Fig. 2(d).

(3) *Proximity to quantum critical point (QCP)*. What is particularly interesting is that for narrow resonances, at moderate to high densities, the boundary detuning $\bar{\nu}_{c,-}(n)$ in Fig. 2(b) nearly aligns with the detuning $\bar{\nu}_c(n)$. This detuning $\bar{\nu}_c(n)$ is associated with a QCP that separates the MSF from the ASF phase. This strong correlation suggests that close proximity to the QCP is a crucial factor in the instability of these narrow resonance molecular superfluids.

To quantitatively confirm the observations above, we present three limiting forms for the scattering lengths $a_{\rm mm}$ and $a^{\rm eff}_{\rm mm}$. These formulas are particularly relevant in the interesting detuning regions where a stable MSF exists and where the compressibility changes its sign [21]. It is important to note that they are applicable only for the magnetic field below the resonance: $B < B_0$.

For a wide resonance at large negative detuning, we find that the scattering lengths $a^{\rm eff}_{\rm mm}$ and $a_{\rm mm}$ are given by

$$a^{\rm eff}_{\rm mm}(n) \approx a_{\rm mm} = a^{\rm bg}_{\rm mm}\left[1 - \left(\frac{\Delta^{\rm wide}_B}{B_0 - B}\right)^2\right], \tag{2a}$$

where $$\Delta^{\rm wide}_B = \frac{\pi}{\sqrt{6}}\sqrt{\frac{\hbar^2}{m_1(\bar{a} - a_{\rm bg})^2\Delta\mu_m}}\Delta B \tag{2b}$$

is an effective molecular resonance width. Here, $a^{\rm bg}_{\rm mm}$, which is chosen to be positive [22], m_1, and $\Delta\mu_m$ are the molecular s-wave background scattering length, the atomic mass, and the magnetic moment difference between the open and closed channels, respectively. As in the literature [5,23], $\bar{a}$ in Eq. (2b) can be taken as $0.96R_{\rm vdW}$, where $R_{\rm vdW}$ is the van der Waals length.

For the narrow resonance case at zero density and with detuning somewhat away from unitarity, we can define a two-body molecular scattering length

$$a_{\rm mm} = a^{\rm bg}_{\rm mm}\left[1 - \left(\frac{\Delta^{\rm narrow}_B}{B_0 - B}\right)^{\frac{3}{2}}\right], \tag{3a}$$

where $$\Delta^{\rm narrow}_B = \left(\frac{a_{\rm bg}}{a^{\rm bg}_{\rm mm}}\right)^{\frac{2}{3}}\left(\frac{m_1 a^2_{\rm bg}\Delta\mu_m}{\hbar^2}\right)^{\frac{1}{3}}(\Delta B)^{\frac{4}{3}} \tag{3b}$$

is the counterpart molecular resonance width. The scattering process underlying the resonant term in Eq. (3a) [24] is illustrated in Fig. 1(b), which involves the exchange of two bosonic atom constituents between molecules. Importantly, the negative sign in front of this term is fundamentally connected to Bose statistics. It can be shown that for a *fermionic* Feshbach resonance, $a_{\rm mm}$ takes a similar form to Eq. (3a), but with the negative sign in front of the resonant term replaced by a *positive* sign (see Refs. [25–27]).

Finally, we present an expression for the many-body molecular scattering length $a^{\rm eff}_{\rm mm}(n)$ in the case of a narrow resonance at finite density,

$$a^{\rm eff}_{\rm mm}(n) \approx a^{\rm bg}_{\rm mm}\left[1 - \left(\frac{\Delta^{\rm narrow}_B}{B_0 - B}\right)^{\frac{3}{2}} f(B,n)\right], \tag{4a}$$

with $$f(B,n) = 1 + \frac{2\sqrt{2}}{\pi}\ln\left(\frac{\bar{\nu}^2}{\bar{\nu}^2 - \bar{\nu}^2_c(n)}\right), \tag{4b}$$

where $\bar{\nu} = \Delta\mu_m(B - B_0)$ is the detuning and $\bar{\nu}_c(n) \approx -2\bar{\alpha}\sqrt{n}$ is its corresponding QCP value, with $\bar{\alpha}$ representing the renormalized Feshbach coupling strength defined in Eq. (6). Equation (4) is applicable for the detuning less than the QCP value, $\bar{\nu} < \bar{\nu}_c < 0$. At zero density, the QCP coincides with the resonance $\bar{\nu}_c = 0$ and Eq. (4a) reduces to Eq. (3) for the two-body scattering length $a_{\rm mm}$.

Qualitatively, one can understand why many-body physics plays an important role in the molecular condensate stability, as the main fluctuations that destabilize the MSF phase in Fig. 2 are atomic Bogoliubov excitations arising from the presence of the ground-state molecular condensate. These excitations exhibit a significant energy gap and behave like free atoms when the detuning is large and negative, as is relevant in a wide resonance. However, they become soft with a phonon-like, low-energy dispersion as the detuning approaches the QCP. For a sufficiently narrow resonance at a given density, it is this softness of the Bogoliubov excitations, rather than proximity to the two-body resonance point, that drives the instability.

These many-body effects are manifested in the logarithmic term in $f(B,n)$ appearing in Eq. (4). This logarithmic dependence has the important consequence that the boundary detuning $\bar{\nu}_{c,-}(n)$ for the narrow resonance is generally exponentially close to the QCP [21]. Importantly, this narrow resonance case presents an interesting opportunity as it provides experimental access to the associated QCP physics from the stable MSF side.

Variational analysis. To arrive at all of these results, we use a variational ground-state analysis that incorporates both atomic and molecular condensates, as well as depletion and atomic Cooper-pairing contributions. Some aspects of these stability issues due to the presence of Cooper pairing of bosons have been discussed in prior work [28–33]. There, the emphasis was primarily restricted to single-channel models.

We adopt a two-channel model Hamiltonian that includes both interchannel Feshbach coupling and intrachannel background interactions:

$$\hat{H} = \sum_{\sigma=1}^{2}\sum_{\mathbf{k}} h_{\sigma\mathbf{k}} a^{\dagger}_{\sigma\mathbf{k}} a_{\sigma\mathbf{k}} - \frac{\alpha}{\sqrt{V}}\sum_{\mathbf{k}_1,\mathbf{k}_2}\left(a^{\dagger}_{1\mathbf{k}_1}a^{\dagger}_{1\mathbf{k}_2}a_{2,\mathbf{k}_1+\mathbf{k}_2} + \text{H.c.}\right) + \sum_{\sigma=1}^{2}\sum_{\mathbf{k}_i}\frac{g_\sigma}{2V}a^{\dagger}_{\sigma\mathbf{k}_1}a^{\dagger}_{\sigma\mathbf{k}_2}a_{\sigma\mathbf{k}_3}a_{\sigma,\mathbf{k}_1+\mathbf{k}_2-\mathbf{k}_3}. \quad (5)$$

Here, $a_{\sigma\mathbf{k}}$ is an annihilation operator for the open-channel atoms (with $\sigma = 1$) or closed-channel molecules ($\sigma = 2$). The summation $V^{-1}\sum_{\mathbf{k}}$, with V the volume, represents an integral over the momentum $\mathbf{k}$ with a cutoff Λ, which is needed to regularize ultraviolet divergences in various $\mathbf{k}$-dependent integrals. Finally, we assume three-dimensional isotropy and ignore trap effects.

In Eq. (5), we define kinetic energy contributions $h_{1\mathbf{k}} = (\hbar\mathbf{k})^2/2m_1 - \mu$ and $h_{2\mathbf{k}} = (\hbar\mathbf{k})^2/2m_2 - (2\mu - \nu)$ with $m_2 = 2m_1$, μ the chemical potential, and ν the *bare* molecule detuning. The parameter $g_\sigma > 0$ corresponds to a *repulsive* intrachannel density-density interaction, and α represents the *bare* Feshbach coupling between the two channels. The parameters $\{\nu, \alpha, g_1, g_2\}$ depend on the cutoff Λ and are related [20,21] to experimental observables by $\nu = \bar{\nu} + \sqrt{2}\beta\alpha\bar{\alpha}$, $\alpha = \bar{\alpha}\Gamma/\sqrt{2}$, $g_1 = \bar{g}_1\Gamma$, and $g_2 = \bar{g}_2/(1 - (2/\pi)\Lambda a^{\text{bg}}_{\text{mm}})$, with $\bar{\alpha} = \sqrt{4\pi\hbar^2 a_{\text{bg}}\Delta\mu_m\Delta B/m_1}$, $\bar{g}_1 = 4\pi\hbar^2 a_{\text{bg}}/m_1 > 0$, $\bar{g}_2 = 4\pi\hbar^2 a^{\text{bg}}_{\text{mm}}/m_2 > 0$, $\beta = m_1\Lambda/(2\pi^2\hbar^2)$, and $\Gamma = 1/(1 - \beta\bar{g}_1)$. These relations are chosen to reproduce the atomic scattering length a_s in Eq. (1) in the two-atom scattering limit. Finally, the momentum cutoff Λ is related to the length scale $\bar{a}$ in Eqs. (2)–(4) by $\Lambda = \pi/(2\bar{a})$.

From the renormalized Feshbach coupling parameter $\bar{\alpha}$, one can define a characteristic length scale r_* [5,25,26,34] as

$$r_* \equiv 4\pi\hbar^4/m_1^2\bar{\alpha}^2 = \hbar^2/(a_{\text{bg}}m_1\Delta\mu_m\Delta B), \quad (6)$$

which allows us to classify the resonance width quantitatively. If the ratio $w_{\text{res}} \equiv a_{\text{bg}}/r_*$ is much smaller than unity ($w_{\text{res}} \ll 1$), the resonance is viewed as narrow; otherwise, it is classified as wide. For the narrow and wide resonances used in this Lettter, we choose $w_{\text{res}} \approx 0.006$ [20,21] and $w_{\text{res}} \sim 1$, respectively [35].

To address the ground-state stability at zero temperature, we adopt the following many-body variational wave function as an approximation to the true ground state of $\hat{H}$:

$$|\Psi_{\text{var}}\rangle = \mathcal{N}^{-1} e^{\sum_\sigma \Psi_{\sigma 0}\sqrt{V}a^{\dagger}_{\sigma 0} + \sum'_{\mathbf{k}}\sum_\sigma \chi_{\sigma\mathbf{k}} a^{\dagger}_{\sigma\mathbf{k}}a^{\dagger}_{\sigma-\mathbf{k}}}|0\rangle, \quad (7)$$

where $\{\Psi_{\sigma 0}, \chi_{\sigma\mathbf{k}}\}$ are the variational parameters and $\mathcal{N}$ is the normalization factor. In the exponent, the $\mathbf{k}$ sum is over half of $\mathbf{k}$ space, and the prime in the $\mathbf{k}$ summation implies that the origin $\mathbf{k} = 0$ is excluded. The vacuum $|0\rangle$ satisfies $a_{\sigma\mathbf{k}}|0\rangle = 0$ for all annihilation operators $a_{\sigma\mathbf{k}}$. In the spirit of generalized Bogoliubov theory, this variational wave function includes only pairwise correlations between atoms or between molecules in the exponent. We emphasize that this approximation is adequate for our focus on the detuning regime that is not too close to the resonance [36]. In Ref. [21], we provide concrete estimates showing that neglecting higher-order correlations results in less than 2% uncertainty in the phase boundaries of the phase diagram in Fig. 2, as well as in the scattering length formulas given in Eqs. (2)–(4).

The trial ground-state energy associated with $|\Psi_{\text{var}}\rangle$ is then

$$\Omega[\Psi_{10}, \Psi_{20}, \chi_{1\mathbf{k}}, \chi_{2\mathbf{k}}] = \langle\Psi_{\text{var}}|\hat{H}|\Psi_{\text{var}}\rangle, \quad (8)$$

which is a functional of the parameters $\{\Psi_{10}, \Psi_{20}, \chi_{1\mathbf{k}}, \chi_{2\mathbf{k}}\}$. Here, $\Psi_{\sigma 0} = \langle a_{\sigma 0}\rangle/\sqrt{V}$ indicates that Ψ_{10} (Ψ_{20}) also represents the amplitude of the atomic (molecular) condensate. Minimizing Ω with respect to $\{\Psi^*_{10}, \Psi^*_{20}, \chi^*_{1\mathbf{k}}, \chi^*_{2\mathbf{k}}\}$ yields a set of saddle-point equations [20]. Those derived from the derivative $\partial\Omega/\partial\chi^*_{\sigma\mathbf{k}}$ can be recast into the form of the BCS-like gap equation by introducing the Cooper-like pairing order parameter $\Delta_\sigma \equiv g_\sigma V^{-1}\sum_{\mathbf{k}\neq 0}\langle a_{\sigma\mathbf{k}}a_{\sigma,-\mathbf{k}}\rangle$. Using the pairing order parameter Δ_σ, one can rewrite the ground-state energy Ω in Eq. (8) as a function of only five unknowns: $\Omega = \Omega[\Psi_{10}, \Psi_{20}, \Delta_1, \Delta_2, \mu]$, whose first-order derivative with respect to the five parameters leads to four saddle-point equations plus one total particle number density constraint: $n = (|\Psi_{10}|^2 + n_1) + 2(|\Psi_{20}|^2 + n_2)$ with $n_\sigma = V^{-1}\sum_{\mathbf{k}\neq 0}\langle a^{\dagger}_{\sigma\mathbf{k}}a_{\sigma\mathbf{k}}\rangle$.

We now numerically solve the five equations. Figures 3(a) and 3(b) plot the calculated chemical potentials near resonance at two different densities for both the wide and narrow resonances. This provides useful insight into the anomalous negative sign of the compressibility and the related condensate instability. From both figures, we observe that the chemical potential μ, which represents the average energy per atom, falls below the two energy levels corresponding to the bare atomic continuum threshold on the atomic side and the two-body molecular energy/2 on the molecular side. Furthermore, as the density n decreases, in the near-resonance regime the chemical potential μ approaches the two energy levels from below. Consequently, the inverse compressibility $\kappa^{-1} = d\mu/dn$ must be *negative* near and on both sides of the resonance [37]. The numerical results that were shown previously in Figs. 2(a) and 2(b) support this analysis; there, we directly evaluated the derivative $d\mu/dn$ numerically, from which we constructed the ground-state stability phase diagrams.

Many-body effective scattering length. Armed with this understanding, we now derive the many-body *effective* scattering

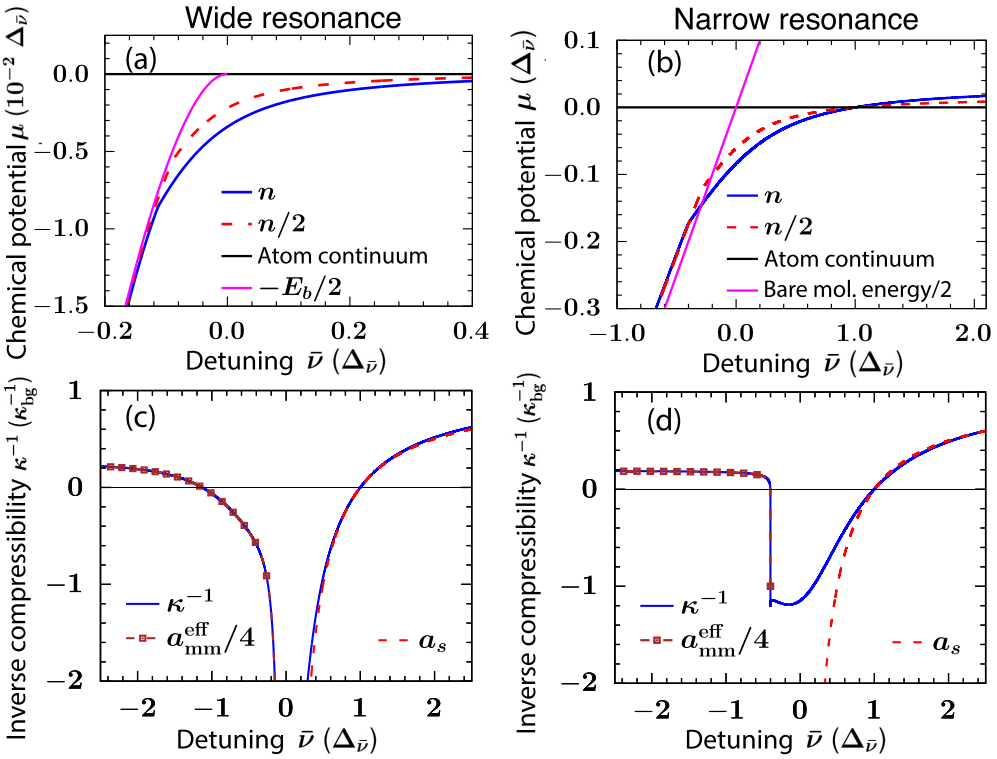

FIG. 3. Chemical potential, inverse compressibility, and molecular scattering lengths. (a), (b) Chemical potential μ (blue solid and red dashed lines) vs detuning $\bar{\nu}$ at densities n and $n/2$, with $na_{\rm bg}^3 = 1.68 \times 10^{-5}$ [same as Figs. 2(c) and 2(d)]. The "atom continuum" threshold is at $\mu = 0$. In panel (a), "$-E_b$" represents the dressed molecular energy; in panel (b), it is replaced by its bare value, $\bar{\nu}$. (c), (d) Comparison of the inverse compressibility (blue solid lines) at $na_{\rm bg}^3 = 1.68 \times 10^{-5}$ with the atomic scattering length a_s (red dashed lines) and the many-body molecular scattering length $a_{\rm mm}^{\rm eff}$ (brown dashed lines with squares), defined in Eq. (9). Both $a_{\rm mm}^{\rm eff}$ and a_s are plotted in units of $a_{\rm bg}$.

length $a_{\rm mm}^{\rm eff}$ for the dressed molecules in terms of an effective interaction $g_2^{\rm eff}$:

$$a_{\rm mm}^{\rm eff}(n) = \frac{m_2}{4\pi\hbar^2} g_2^{\rm eff}(n), \tag{9a}$$

$$\text{with} \qquad g_2^{\rm eff} = \frac{(\mathcal{Z}^{\rm eff})^2}{2} \frac{\partial^4 \Omega[\Psi_{10}, \Psi_{20}, \Delta_1, \Delta_2, \mu]/V}{\partial \Psi_{20}^2 \partial (\Psi_{20}^*)^2}. \tag{9b}$$

Here, $\mathcal{Z}^{\rm eff}$ is the fraction of the dressed-molecular condensate in the closed channel, defined by $\mathcal{Z}^{\rm eff} = |\Psi_{20}|^2/(|\Psi_{20}|^2 + n_1/2)$ [38]. The quartic derivative in Eq. (9b) can be carried out approximately [21, 39], leading to

$$\frac{g_2^{\rm eff}}{(\mathcal{Z}^{\rm eff})^2} \approx \widetilde{\bar{g}}_2 - \widetilde{\bar{\alpha}}^4 \left[\frac{1}{V} \sum_{\mathbf{k}} \frac{1}{2E_{1\mathbf{k}}^3} - 2g_1 \left(\frac{1}{V} \sum_{\mathbf{k}} \frac{\widetilde{\epsilon}_{1\mathbf{k}}}{2E_{1\mathbf{k}}^3} \right)^2 \right], \tag{10}$$

where $E_{1\mathbf{k}} = \sqrt{\widetilde{\epsilon}_{1\mathbf{k}}^2 - |\widetilde{\Delta}_1|^2}$ is the atomic Bogoliubov quasiparticle energy, with $\widetilde{\epsilon}_{1\mathbf{k}} = h_{1\mathbf{k}} + 2g_1(|\Psi_{10}|^2 + n_1)$ and $\widetilde{\Delta}_1 = \Delta_1 + g_1\Psi_{10}^2 - 2\alpha\Psi_{20}$. In Eq. (10), $\widetilde{\bar{\alpha}}$ and $\widetilde{\bar{g}}_2$ are two interaction parameters, related to the Feshbach coupling $\bar{\alpha}$ and molecule-molecule interaction $\bar{g}_2$ by $\widetilde{\bar{\alpha}} = \sqrt{2}\alpha/(1 + g_1 V^{-1} \sum_{\mathbf{k}} 1/2E_{1\mathbf{k}})$ and $\widetilde{\bar{g}}_2 = g_2/(1 + g_2 V^{-1} \sum_{\mathbf{k}} 1/2E_{2\mathbf{k}})$. It is important to note that Eq. (10) is applicable as long as the detuning $\bar{\nu}$ is smaller than and not too close to its QCP value $\bar{\nu}_c$ as we have already set $\Psi_{10} = 0$. Evaluating Eqs. (9) and (10) leads to the $a_{\rm mm}^{\rm eff}$ plots in Figs. 2(c) and 2(d).

The overall minus sign associated with the term $\sum_{\mathbf{k}} 1/2E_{1\mathbf{k}}^3$ in Eq. (10) should be noted. This term arises from contributions related to the scattering process shown in Fig. 1(b). It should be clear that the presence of $E_{1\mathbf{k}}$ in the denominator reflects the fact that the excitations involved in the intermediate scattering state are atomic Bogoliubov quasiparticles.

In general, the $\mathbf{k}$ integral in Eq. (10) cannot be done analytically. However, for the narrow resonance case and detuning near the QCP, Eqs. (10) and (9) can be further simplified to yield the simple analytical expression for the many-body scattering length $a_{\rm mm}^{\rm eff}$ [21] presented in Eq. (4). In Figs. 3(c) and 3(d), we numerically evaluate $a_{\rm mm}^{\rm eff}$ for a generic detuning in both the narrow and wide resonance cases, and compare it with the numerically calculated compressibility inverse κ^{-1} [40]. Notably, the two, $a_{\rm mm}^{\rm eff}$ and κ^{-1}, show rather precise agreement, for both the narrow and wide resonances at detunings away from the immediate vicinity of the QCP [41].

All of this allows us to understand why the compressibility in Figs. 2(a) and 2(b) behaves so differently when comparing the behavior of wide and narrow resonances. For a very narrow resonance, because of the small Feshbach coupling $\bar{\alpha}$, the factor $\widetilde{\bar{\alpha}}^4$ in Eq. (10), which is proportional to $\bar{\alpha}^4$, is very small. Consequently, the effective scattering length $a_{\rm mm}^{\rm eff}$ becomes negative only when the atomic Bogoliubov quasiparticle energy gap (contained in $E_{1\mathbf{k}=0}$) is sufficiently small. This ensures that the detuning at which $a_{\rm mm}^{\rm eff}$ changes sign is sufficiently close to the QCP. In contrast, for a wide

resonance, this occurs when the gap $E_{1\mathbf{k}=0}$ is still large, which corresponds to a detuning well away from the QCP.

Zero-density limit. The expressions for the two-body scattering length $a_{\rm mm}$, presented in Eqs. (2) and (3), were obtained from the zero-density limit of $a_{\rm mm}^{\rm eff}$ in Eq. (9), which leads to

$$a_{\rm mm} = a_{\rm mm}^{\rm bg} - \frac{a_{\rm mm}^{\rm bg}}{k_b^4 r_* \bar{a}^3} A_1 - \frac{1}{k_b^6 r_*^2 \bar{a}^3} A_2 + \frac{a_{\rm bg}}{k_b^8 r_*^2 \bar{a}^6} A_3, \quad (11)$$

where r_* was defined in Eq. (6) and $k_b = \sqrt{mE_b}/\hbar$ is the detuning-dependent momentum corresponding to the molecular binding energy E_b. The three dimensionless and positive coefficients $\{A_1, A_2, A_3\}$ contain subleading dependences on $1/k_b$ [21], and their expressions are given in Supplemental Material [21]. To arrive at Eqs. (2) and (3), we retain the background contribution $a_{\rm mm}^{\rm bg}$ in Eq. (11) along with the A_1 and A_2 terms, which are dominant for the wide and narrow resonances, respectively, near the boundary detuning $\bar{\nu}_{c,-}$ in Fig. 2.

Conclusions. In this Letter, we have conducted an in-depth study on the stability of molecular condensates near Feshbach resonances in bosonic atoms, establishing the relationship to the intermolecular scattering lengths. In contrast with the Fermi gases, there has, thus far, been very little theoretical work on characterizing this property for those molecules comprised of bosonic atoms. Such calculations cannot naturally build on past work for the Fermi systems [42], as in the Bose problem in the more immediate vicinity of resonance, one has to contend with Efimov and tetramer bound states as well as other background contributions. With the caveat that, following experiment [6,7], we are not too close to resonance (where instability is guaranteed), we have shown how just as Feshbach resonances allow tuning of the scattering lengths of atoms, they also modify the scattering length of molecules constituted from these atoms.

Our predictions are ripe for experimental validation. The concrete expressions for the molecular scattering lengths we derived make it possible to address a number of issues that were previously inaccessible; these include, among others, the equilibrium equation of state in the dilute molecular gas regime, the expansion dynamics, the collective modes, and the molecule-molecule scattering-induced relaxation [13,26, 42–44].

Acknowledgments. We thank P. Julienne and B. Zhao for helpful discussions. Z.W. and Q.C. were supported by the Innovation Program for Quantum Science and Technology (Grant No. 2021ZD0301904). This work was also supported by the National Science Foundation under Grants No. PHY-2409612 and No. PHY-2103542, and by the Air Force Office of Scientific Research under Award No. FA9550-21-1-0447. Z.Z. acknowledges the Bloch Postdoctoral Fellowship. We also acknowledge the University of Chicago's Research Computing Center for their support of this work.

Data availability. The data supporting this study's findings are available within the Letter.

[1] L. Radzihovsky, J. Park, and P. B. Weichman, Superfluid transitions in bosonic atom-molecule mixtures near a Feshbach resonance, Phys. Rev. Lett. **92**, 160402 (2004).

[2] M. W. J. Romans, R. A. Duine, S. Sachdev, and H. T. C. Stoof, Quantum phase transition in an atomic Bose gas with a Feshbach resonance, Phys. Rev. Lett. **93**, 020405 (2004).

[3] L. Radzihovsky, P. B. Weichman, and J. I. Park, Superfluidity and phase transitions in a resonant Bose gas, Ann. Phys. **323**, 2376 (2008).

[4] L. Radzihovsky and S. Choi, *P*-wave resonant Bose gas: A finite-momentum spinor superfluid, Phys. Rev. Lett. **103**, 095302 (2009).

[5] C. Chin, R. Grimm, P. Julienne, and E. Tiesinga, Feshbach resonances in ultracold gases, Rev. Mod. Phys. **82**, 1225 (2010).

[6] Z. Zhang, L. Chen, K.-X. Yao, and C. Chin, Transition from an atomic to a molecular Bose–Einstein condensate, Nature (London) **592**, 708 (2021).

[7] Z. Zhang, S. Nagata, K. Yao, and C. Chin, Many-body chemical reactions in a quantum degenerate gas, Nat. Phys. **19**, 1466 (2023).

[8] P. O. Fedichev, M. W. Reynolds, and G. V. Shlyapnikov, Three-body recombination of ultracold atoms to a weakly bound *s* level, Phys. Rev. Lett. **77**, 2921 (1996).

[9] P. F. Bedaque, E. Braaten, and H.-W. Hammer, Three-body recombination in Bose gases with large scattering length, Phys. Rev. Lett. **85**, 908 (2000).

[10] T. Weber, J. Herbig, M. Mark, H.-C. Nägerl, and R. Grimm, Three-body recombination at large scattering lengths in an ultracold atomic gas, Phys. Rev. Lett. **91**, 123201 (2003).

[11] R. J. Fletcher, A. L. Gaunt, N. Navon, R. P. Smith, and Z. Hadzibabic, Stability of a unitary Bose gas, Phys. Rev. Lett. **111**, 125303 (2013).

[12] D. S. Petrov, C. Salomon, and G. V. Shlyapnikov, Weakly bound dimers of fermionic atoms, Phys. Rev. Lett. **93**, 090404 (2004).

[13] D. S. Petrov, C. Salomon, and G. V. Shlyapnikov, Scattering properties of weakly bound dimers of fermionic atoms, Phys. Rev. A **71**, 012708 (2005).

[14] W. Zwerger, The BCS-BEC Crossover and the Unitary Fermi Gas in *Lecture Notes in Physics* (Springer-Verlag, Berlin, 2012), Vol. 836.

[15] C. A. Regal, M. Greiner, and D. S. Jin, Observation of resonance condensation of fermionic atom pairs, Phys. Rev. Lett. **92**, 040403 (2004).

[16] M. W. Zwierlein, C. A. Stan, C. H. Schunck, S. M. F. Raupach, A. J. Kerman, and W. Ketterle, Condensation of pairs of fermionic atoms near a Feshbach resonance, Phys. Rev. Lett. **92**, 120403 (2004).

[17] Q. Chen, J. Stajic, S. Tan, and K. Levin, BCS–BEC crossover: From high temperature superconductors to ultracold superfluids, Phys. Rep. **412**, 1 (2005).

[18] While higher-order contributions, involving repeated processes from Fig. 1(a), renormalize B_0, they do not change the resonant structure of a_s.

[19] The formulas derived here can be easily generalized to the case of negative ΔB.

[20] Z. Wang, K. Wang, Z. Zhang, S. Nagata, C. Chin, and K. Levin, Stability and dynamics of atom-molecule superfluids

near a narrow Feshbach resonance, Phys. Rev. A **110**, 013306 (2024).

[21] See Supplemental Material at http://link.aps.org/supplemental/10.1103/r2gt-gcyt for additional details, including derivations of the molecular scattering length formulas, variational analysis, estimates of phase-boundary uncertainties, and further results for a fermionic Feshbach resonance. References [45–58] are also provided therein.

[22] In this Letter, we consider only the case where both $a_{\rm bg}$ and $a_{\rm mm}^{\rm bg}$ are positive.

[23] A. D. Lange, K. Pilch, A. Prantner, F. Ferlaino, B. Engeser, H.-C. Nägerl, R. Grimm, and C. Chin, Determination of atomic scattering lengths from measurements of molecular binding energies near Feshbach resonances, Phys. Rev. A **79**, 013622 (2009).

[24] Note that the whole contribution of the resonance term in Eq. (3a) does not depend on $a_{\rm mm}^{\rm bg}$, since the overall prefactor of $a_{\rm mm}^{\rm bg}$ is canceled out by a factor of $1/a_{\rm mm}^{\rm bg}$ from $(\Delta_B^{\rm narrow})^2$.

[25] V. Gurarie and L. Radzihovsky, Resonantly paired fermionic superfluids, Ann. Phys. **322**, 2 (2007).

[26] J. Levinsen and D. S. Petrov, Atom-dimer and dimer-dimer scattering in fermionic mixtures near a narrow Feshbach resonance, Eur. Phys. J. D **65**, 67 (2011).

[27] On the other hand, in the fermionic studies of Refs. [25,26], the effect of the molecular background interaction $a_{\rm mm}^{\rm bg}$ on $a_{\rm mm}$ was not considered. For additional discussions, see Ref. [21].

[28] W. Evans and Y. Imry, On the pairing theory of the Bose superfluid, Nuovo Cimento B **63**, 155 (1969).

[29] P. Nozieres and D. Saint James, Particle vs pair condensation in attractive Bose liquids, J. Phys. France **43**, 1133 (1982).

[30] G. S. Jeon, L. Yin, S. W. Rhee, and D. J. Thouless, Pairing instability and mechanical collapse of a Bose gas with an attractive interaction, Phys. Rev. A **66**, 011603(R) (2002).

[31] A. Koetsier, P. Massignan, R. A. Duine, and H. T. C. Stoof, Strongly interacting Bose gas: Nozières and Schmitt-Rink theory and beyond, Phys. Rev. A **79**, 063609 (2009).

[32] Y.-L. Lee and Y.-W. Lee, Universality and stability for a dilute Bose gas with a Feshbach resonance, Phys. Rev. A **81**, 063613 (2010).

[33] S. Basu and E. J. Mueller, Stability of bosonic atomic and molecular condensates near a Feshbach resonance, Phys. Rev. A **78**, 053603 (2008).

[34] T.-L. Ho, X. Cui, and W. Li, Alternative route to strong interaction: Narrow Feshbach resonance, Phys. Rev. Lett. **108**, 250401 (2012).

[35] We note that using an even wider resonance does not change our conclusions. We use the moderately wide resonance to make our numerical calculation easier.

[36] K. Wang, Z. Zhang, S. Nagata, Z. Wang, and K. Levin, Universal coherent atom-molecule oscillations in the dynamics of the unitary Bose gas near a narrow Feshbach resonance, Phys. Rev. Res. **7**, L012025 (2025).

[37] In contrast to the near-resonance regime in Figs. 3(a) and 3(b), the chemical potential μ rises above one of the two energy levels when the detuning is far off the resonance. This is true for both the wide- and narrow-resonance cases (see Ref. [21] for additional details). It implies that, in these far-off-resonance regimes, the chemical potential must approach these levels from above as the density vanishes ($n \to 0$), consistent with the fact that the compressibility is positive in those detuning regimes.

[38] The factor $(\mathcal{Z}^{\rm eff})^2$ in Eq. (9b) is needed to reconcile two facts: (1) the many-body scattering length $a_{\rm mm}^{\rm eff}$, as well as the two-body one $a_{\rm mm}$, is defined for a *dressed* molecule [21], which is an admixture of closed-channel molecules with open-channel atom pairs, and (2) the derivative in Eq. (9b) is taken with respect to the *bare* closed-channel molecular condensate amplitude Ψ_{20}. Although this factor is essentially equal to 1 for a narrow resonance, it becomes important for wide resonances, particularly in deriving Eq. (2) [21] in the zero-density limit.

[39] When performing derivatives in Eq. (9b), we set $\{\Psi_{10}, \Delta_1, \Delta_2\}$ at their saddle-point values. They are viewed as functions of $\{\Psi_{20}, \mu\}$ only. In arriving at Eq. (10), we have also neglected terms that are higher order in the ratios $\{g_1 n/E_{1\mathbf{k}=0}, g_2 n/E_{1\mathbf{k}=0}, \alpha\sqrt{n}/E_{1\mathbf{k}=0}\}$.

[40] At large negative detuning $\bar{\nu}$, the many-body scattering length $a_{\rm mm}^{\rm eff}$ approaches its two-body background counterpart $a_{\rm mm}^{\rm bg}$.

[41] We note that the more extended unstable regime in Fig. 2(a) for a wide resonance is associated with the presence of a sizable number of atom Cooper pairs [21], which is also a consequence of the larger Feshbach coupling strength $\bar{\alpha}$.

[42] J. Levinsen and V. Gurarie, Properties of strongly paired fermionic condensates, Phys. Rev. A **73**, 053607 (2006).

[43] C. Chin, T. Kraemer, M. Mark, J. Herbig, P. Waldburger, H.-C. Nägerl, and R. Grimm, Observation of Feshbach-like resonances in collisions between ultracold molecules, Phys. Rev. Lett. **94**, 123201 (2005).

[44] X.-Y. Chen, A. Schindewolf, S. Eppelt, R. Bause, M. Duda, S. Biswas, T. Karman, T. Hilker, I. Bloch, and X.-Y. Luo, Field-linked resonances of polar molecules, Nature (London) **614**, 59 (2023).

[45] Y. Ohashi and A. Griffin, BCS-BEC crossover in a gas of Fermi atoms with a Feshbach resonance, Phys. Rev. Lett. **89**, 130402 (2002).

[46] B. Marcelis, E. G. M. van Kempen, B. J. Verhaar, and S. J. J. M. F. Kokkelmans, Feshbach resonances with large background scattering length: Interplay with open-channel resonances, Phys. Rev. A **70**, 012701 (2004).

[47] G. M. Falco and H. T. C. Stoof, Dressed molecules in resonantly interacting ultracold atomic Fermi gases, Phys. Rev. A **75**, 023612 (2007).

[48] J. M. Gerton, D. Strekalov, I. Prodan, and R. G. Hulet, Direct observation of growth and collapse of a Bose–Einstein condensate with attractive interactions, Nature (London) **408**, 692 (2000).

[49] D. S. Petrov, Three-boson problem near a narrow Feshbach resonance, Phys. Rev. Lett. **93**, 143201 (2004).

[50] R. A. Duine and H. T. C. Stoof, Atom–molecule coherence in Bose gases, Phys. Rep. **396**, 115 (2004).

[51] A. J. Leggett, The relation between the Gross–Pitaevskii and Bogoliubov descriptions of a dilute Bose gas, New J. Phys. **5**, 103 (2003).

[52] J. Stajic, J. N. Milstein, Q. Chen, M. L. Chiofalo, M. J. Holland, and K. Levin, Nature of superfluidity in ultracold Fermi gases near Feshbach resonances, Phys. Rev. A **69**, 063610 (2004).

[53] I. V. Brodsky, M. Y. Kagan, A. V. Klaptsov, R. Combescot, and X. Leyronas, Exact diagrammatic approach for dimer-dimer

scattering and bound states of three and four resonantly interacting particles, Phys. Rev. A **73**, 032724 (2006).

[54] P. Pieri and G. C. Strinati, Strong-coupling limit in the evolution from BCS superconductivity to Bose-Einstein condensation, Phys. Rev. B **61**, 15370 (2000).

[55] S. Tan and K. Levin, Modified many-body wave function for BCS-BEC crossover in Fermi gases, Phys. Rev. A **74**, 043606 (2006).

[56] A. O. Gogolin, C. Mora, and R. Egger, Analytical solution of the bosonic three-body problem, Phys. Rev. Lett. **100**, 140404 (2008).

[57] J. P. D'Incao, J. von Stecher, and C. H. Greene, Universal four-boson states in ultracold molecular gases: Resonant effects in dimer-dimer collisions, Phys. Rev. Lett. **103**, 033004 (2009).

[58] G. M. Falco and H. T. C. Stoof, Atom-molecule theory of broad Feshbach resonances, Phys. Rev. A **71**, 063614 (2005).